Available online at www.sciencedirect.com
SCIENCE DIRECT
Coastal Engineering 53 (2006) 243 – 254
Coastal Engineering
An International Journal for Coastal, Harbour and Offshore Engineers
www.elsevier.com/locate/coastaleng

Wave driven alongshore sediment transport and stability of the Dutch coastline

A. Falqués

Applied Physics Department, Technical University of Catalonia, Spain

Available online 13 December 2005

Abstract

The wave-driven alongshore sediment transport is commonly supposed to smooth out the irregularities on the coastline. However, it has been shown that waves approaching the coast with a high angle with respect the shore-normal can reverse that tendency and cause the rectilinear coast to be unstable [Ashton, A., Murray, A.B., Arnault, O., 2001. Formation of coastline features by large-scale instabilities induced by high-angle waves, Nature 414, 296–300. Falqués, A., Calvete, D. Large scale dynamics of sandy coastlines. Diffusivity and instability, J. Geophys. Res., 110, 2005, doi:10.1029/2004JC002587]. The extended one-line coastline model presented in the latter paper is here applied to investigate the stability of the Dutch coast. The main aim is testing the hypothesis that the shoreline sand waves observed along this coast could be generated by such an instability. It is found that the Dutch coast has potential for instability. This is most prominent on the Holland coast, followed by the Delta coast and is very weak on the Wadden coast. Whether the instability actually occurs or not depends on the cross-shore bathymetric profile of the shoreline waves. Under the sensible assumption that the bathymetric perturbation is just a shift of the equilibrium beach profile, the Dutch coast is stable. In this case, the mean annual coastline diffusivity is evaluated and it is found to be typically about 0.010–0.015 $m^2\ s^{-1}$, that is, roughly smaller by a factor 2 than that predicted by the traditional one-line model. However, the Dutch coast may be unstable with respect to coastline waves with a maximum bathymetric signal at a few hundred meters from the coast. This is shown in one case where the shoals associated with the sand wave are inside the surf zone during moderate storm waves. Thus the sand waves could result from the cross-shore redistribution of the sand associated with an alongshore series of shoals and bed depressions generated by the alongshore transport in the surf zone. While the generation or not of such shoreline waves by this instability strongly depends on their profile, its propagation once they have been created is less sensitive and is well reproduced by the present model. It is explained why the propagation is to the NE along the Delta and Wadden coasts, why it is faster on the latter and why on the Holland coast there is no clear propagation direction.

PACS: 92.10.Sx; 92.10.Wa; 91.50.Cw; 92.10.Hm; 47.20.Hw
Keywords: Dutch coast; Alongshore sediment transport; Shoreline sand waves; Coastline instabilities; Coastline diffusivity; High angle waves

1. Introduction

The one-line modelling is a well known tool in Coastal Engineering to predict changes in coastline position due to the wave driven sediment transport along the coast (Pelnard-Considère, 1956; Horikawa, 1988; Komar, 1998). It is however a severe simplification of nearshore morphodynamics which is, in fact, 3D. It consists in averaging on the vertical and the cross-shore directions so that the morphodynamically active region collapses in a single line which represents the coastline. The changes in coastline position are then given by convergence/divergence of the total alongshore sediment transport rate Q which is determined just by the wave forcing without account of surf zone hydrodynamics (water inertia, mass conservation, etc.). Cross-shore sediment transport is usually not explicitly considered. However, cross-shore transport is always implicitly present via the sediment redistribution that is necessary to reach the equilibrium beach profile after the changes which are driven by alongshore transport. Despite all those simplifications, the one-line modelling has been used for years by coastal engineers and has proven to have reasonable skill for coastline evolution prediction at large time and space scales (years and kilometers) (Larson et al., 1987; Larson and Kraus, 1991).

In the simplest version of one-line modelling, the governing equation for the small deviations of the coastline position with respect to its rectilinear trend is a linear diffusion equation. The diffusivity is positive provided that the angle between wave

E-mail address: falques@fa.upc.es.

0378-3839/$ - see front matter © 2005 Elsevier B.V. All rights reserved.
doi:10.1016/j.coastaleng.2005.10.012

fronts and the coastline at breaking is smaller than 45°. Since this is typically the case because of the refraction of the waves as they approach the coast, the diffusivity in this model is always positive (Falqués, 2003; Falqués and Calvete, 2005). This has the important implication that the rectilinear coastline is stable, any perturbation tending to diffuse away. In contrast, Ashton et al. (2001) have shown that, even if the wave angle at breaking is smaller than 45°, when the angle in deep water is larger than about 42° the rectilinear coastline is unstable. This means that the alongshore sediment transport, rather than smoothing the irregularities in the rectilinear trend of the coastline, may cause the growth of sand waves, capes and spits. This is therefore in disagreement with the predictions of the traditional one-line modelling.

On the other hand, it is known that shoreline features can move downdrift as 'sand waves' when there is a predominant littoral drift along the coast. The propagation of shoreline sand waves, i.e., undulations of the coastline, has been reported from many coasts (see, for instance, Bruun (1954), Bakker (1968), Inman (1987), Verhagen (1989), Stewart and Davidson-Arnott (1988), Larson and Kraus (1991), Thevenot and Kraus (1995), Guillen et al. (1999), Stive et al. (2002), Ruessink and Jeuken (2002) and the review in Falqués (2002)). However, if the governing equation for coastline dynamics would be a diffusion one without advection terms it would be no appropriate to describe the propagation of sand waves except in very particular situations (e.g., forced features, see Bakker (1968)). Thus, the absence of advection terms is another important limitation of the traditional one-line model.

Falqués and Calvete (2005) have recently shown that the one-line model can be easily extended to allow for both shoreline instabilities and propagation of sand waves but, at the same time, keeping the attractive one-line concept. The key point for this extension is the following. Any change in coastline position is necessarily linked to changes in nearshore bathymetry which affect the wave transformation from deep water up to breaking. Thus, the changes in coastline position do affect the wave height and direction at breaking which are needed to compute the alongshore sediment transport rate. In the traditional model leading to the diffusion equation these changes in wave transformation are disregarded. In contrast, the new model considers, in some simplified way, the changes in nearshore bathymetry associated with coastline dynamics and computes the wave transformation accordingly. This effect was already shown by Ashton et al. (2001) to be essential for the 'High angle-waves instability'. However, the main differences between both models are the following. In Ashton et al. (2001), when a stretch of coastline changes orientation, the waves arriving at it are transformed by assuming rectilinear bottom contours which are all parallel to that stretch of coastline. Also, the changes in bathymetry associated with changes in coastline orientation are assumed to extend up to deep water. In contrast, in Falqués and Calvete (2005) the bottom contours are assumed to be curvilinear and the perturbations in bathymetry associated with shoreline changes are assumed to extend only up to a certain finite offshore distance. Another important difference between both models is that Falqués and Calvete (2005) examines small amplitude coastline features (linear stability) while Ashton et al. (2001) uses a nonlinear model so as there is no small amplitude restriction. Another related paper, Falqués (2003), is based on the same assumptions as Ashton et al. (2001) but focuses on the coastline diffusivity for small amplitude features rather than on coastline instability.

An interesting feature of Falqués and Calvete (2005), not predicted by Ashton et al. (2001), is that the instability caused by high angle-waves has a preferred wavelength at which shoreline features initially develop. This wavelength, λ, scales with the width of the surf zone, X_b, but with a large factor $\lambda/X_b \sim 40-150$. It is typically about 4–15 km, i.e., one or two orders of magnitude larger than the spacing of surf zone rhythmic features (van Enckevort et al., 2004). Intriguingly, this is the same range of the wavelengths of the shoreline sand waves observed along the Dutch coast (Verhagen, 1989; Guillen et al., 1999; Ruessink and Jeuken, 2002). This coincidence suggests that the 'High angle-waves instability' could be the cause of such sand waves. This is reasonable as SW and N–NW waves are dominant and arrive at the coast with a large angle. A preliminary study by Ashton et al. (2003) pointed out that the wave obliqueness is moderate suggesting that the Dutch coast is at the threshold for High angle-waves instability, hereinafter referred to as HAWI. This would be consistent with the small amplitude (a few tens of meters, while the wavelengths are of kilometers) of those sand waves. There is therefore a clear motivation to perform a stability analysis of the Dutch coast under the wave driven alongshore sediment transport.

The description of shoreline sand waves along the Dutch coast in the literature is summarized in Section 2. Although the extended one-line model has already been presented in Falqués and Calvete (2005) we briefly outline it in Section 3. Furthermore, the details of the statistical adaptation of the model are presented here. The application of the model to the Dutch coast is described in Section 4. Little is known about the cross-shore structure of the sand waves so that some assumptions have to be made. Stability is analyzed in Section 5 by assuming that the bathymetric perturbation associated with the sand wave corresponds just to a cross-shore shift of the equilibrium profile. The effects of assuming a maximum bathymetric perturbation at some distance from the coast is explored in Section 6. The results are discussed in Section 7 and the final conclusions are presented in Section 8.

2. Observation of shoreline sand waves along the Dutch coast

With various techniques, Bakker (1968), Verhagen (1989), Guillen et al. (1999) and Ruessink and Jeuken (2002) have detected, after removing the mean trends, the propagation of waves on the coastline position along the Dutch coast. According to Ruessink and Jeuken (2002), the wavelength is about 3.5–10 km and the amplitudes are small, ranging from $A=20$ to 50 m. The celerity ranges between 0 and 0.2 km/yr. Looking at Figs. 1, 3 and 6 of that paper, it becomes apparent that on the southern part (Delta coast) there is a clear northward propagation at about 0.07 km/yr. On the central coast (Holland)

this becomes unclear: most of the waves seem stationary, but some of them seem to go on northward whereas some of them seem to propagate southward. It depends on the location and on the time period, southward propagation being apparent only during the last 50 years. This is also consistent with results of Guillen et al. (1999) who analyzed the Jarkus data set during the period 1964–1992 and found southward propagation of sand waves along the Holland coast. Their wavelength is however quite short, $\lambda \sim 2-3$ km, and the celerity is $V \simeq 0.15-0.2$ km/yr. In the northern stretch of the coast (Wadden coast), there is again a clear propagation to the northeast with a celerity of about 0.13 km/yr, which is clearly higher than on the delta coast. The results of the analysis by Verhagen (1989) are qualitatively in agreement with Ruessink and Jeuken (2002) but some quantitative differences arise. Larger sand wave amplitudes ranging from 30 to 500 m are reported and the wavelengths are larger too, ranging from 2.5 up to 22 km. Hereinafter we will refer to the position of shoreline advance or cusp as a crest of the wave and to the shoreline retreat or embayment as through of the wave.

3. Extended one-line model

3.1. Stability under steady wave conditions

The stability of the coast is first examined by considering constant offshore wave conditions given by a single monochromatic wave train with constant $H=H_{\mathrm{rms}}$ and $T=T_{\mathrm{p}}$. How the formulation can be extended such that it also accounts for intra-annual variability associated with a wave climate is shown in Section 3.2.

A Cartesian coordinate system is assumed, x seawards in the cross-shore direction, y running alongshore and z upwards along the vertical. The aim is a description of the dynamics of the small departures of the coastline with respect to its rectilinear trend given by the y-axis. The dynamics of the coastline is described by the sediment conservation:

$$\bar{D}\,\frac{\partial x_{\mathrm{s}}}{\partial t} = -\frac{\partial Q}{\partial y} \tag{1}$$

where Q is the total sediment transport rate ($\mathrm{m^3\ s^{-1}}$) in the y direction, t is time and the perturbed coastline is given by $x=x_{\mathrm{s}}(y,t)$ (Pelnard-Considère, 1956; Horikawa, 1988; Komar, 1998). The mean active water depth $\bar{D}$ is of the order of the depth of closure, D_{c}, and a precise definition of it is given in Falqués and Calvete (2005). An extension of the widely used CERC formula (Komar, 1998; Horikawa, 1988) is considered for the sediment transport rate:

$$Q = \mu H_{\mathrm{b}}^{5/2}\left(\sin(2\alpha_{\mathrm{b}}) - \frac{2r}{\beta}\cos(\alpha_{\mathrm{b}})\frac{\partial H_{\mathrm{b}}}{\partial y}\right) \tag{2}$$

where H_{b} is the (rms) wave height and α_{b} is the angle between wave fronts and coastline at breaking (see Fig. 1). The constant in front of it is of order $\mu \sim 0.1-0.2\ \mathrm{m^{1/2}\ s^{-1}}$ and β is the beach slope at the shoreline. The value $r=1$ has been used (Horikawa, 1988).

The computation of sediment transport with Eq. (2) requires the previous knowledge of $H_{\mathrm{b}}(y,t)$ and $\alpha_{\mathrm{b}}(y,t)$ which are computed by performing wave transformation from deep water. This is done by solving the wave front conservation and energy conservation equations together with the dispersion relation (Mei, 1989; Horikawa, 1988)

$$\frac{\partial k_y}{\partial x} - \frac{\partial k_x}{\partial y} = 0 \quad , \quad \nabla\cdot\left(H^2\vec{c}_{\mathrm{g}}\right) = 0 \quad , \quad \omega^2 = gk\tanh(kD) \tag{3}$$

and boundary conditions in deep water, $H(x_\infty,y,t)=H_\infty(y,t)$, $\theta(x_\infty,y,t)=\theta_\infty(y,t)$, where $x=x_\infty$ is an offshore position. The wave direction is measured by the angle between the wave rays and the $-x$ axis, represented by $-\theta$ and defined by $k_x=-k\cos\theta(x,y)$, $k_y=k\sin\theta(x,y)$ where $\vec{k}$ is the wavevector (see Fig. 1). If the angle between the coastline and the y-axis is $\arctan(\partial x_{\mathrm{s}}/\partial y)=\phi$, the angle between wave fronts and bathymetric contours at breaking will be $-\alpha_{\mathrm{b}}=-\theta_{\mathrm{b}}(y,t)+\phi(y,t)$. The group velocity and the frequency are $\vec{c}_{\mathrm{g}}$ and ω, D is the water depth and g is gravity. Thus, the governing equations of the morphodynamic system are Eqs. (1-3) with the boundary conditions in deep water and sediment flux, Eq. (2).

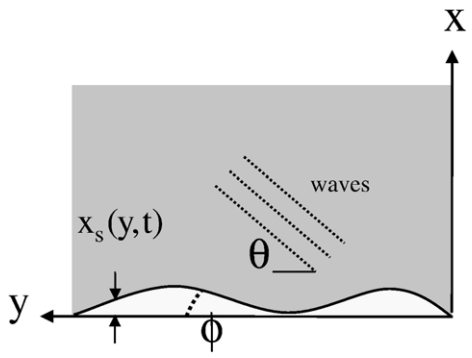

Fig. 1. Sketch of the geometry and the variables. The angle between the wave fronts and the local shoreline is $\alpha=\theta-\phi$.

We will now derive the equation governing the dynamics of small perturbations of the rectilinear coastline, $x=x_{\mathrm{s}}(y,t)$. Formally, the procedure is a linear stability analysis of the basic reference state corresponding to the rectilinear coastline. Given an alongshore uniform topography $D=D_0(x)$ with $D_0(0)=0$ and a steady and uniform deep water wave input, $H_\infty(y,t)=$const., $\theta_\infty(y,t)=$const., this basic state is immediately found as a steady and alongshore uniform solution of our system

$$x_{\mathrm{s}} = 0, \quad k = k_0(x), \quad \theta = \theta_0(x), \quad H = H_0(x). \tag{4}$$

Let us now consider a small deviation of the rectilinear coastline given by $x_{\mathrm{s}}(y,t)$. Associated with it we will assume a topographic perturbation with total water depth given by:

$$D(x,y,t) = D_0(x) - h(x,y,t) = D_0(x) - \beta f(x) x_{\mathrm{s}}(y,t) \tag{5}$$

with a shape function $f(x)$ that verifies $f(0)=1$. The departure from rectilinear and parallel depth contours defined by Eq. (5) induces a perturbation on the wave properties:

$$k = k_0(x) + k'(x,y,t),\ \theta = \theta_0(x) + \theta'(x,y,t),$$
$$H = H_0(x) + H'(x,y,t). \tag{6}$$

Once the perturbed wave properties are known, the quantities defined at the breaking line which are needed to compute sediment transport can be computed. From the equation defining the position of the breaker line, $H(x_b)=\gamma_b D(x_b)$, where γ_b is the breaking index, the perturbed breaking line is evaluated. This permits determination of the perturbations in wave angle and wave height at the perturbed breaking line. Finally, owing to the linearized relationship $\alpha_b=\theta_b-\phi\simeq\theta_b-\partial x_s/\partial y$ the morphodynamic governing equation

$$\frac{\partial x_s}{\partial t}=\frac{2\mu\left(H_b^0\right)^{5/2}}{\bar{D}}\left(\left(\frac{\partial^2 x_s}{\partial y^2}-\frac{\partial\theta_b'}{\partial y}\right)\cos\left(2\theta_b^0\right)-\frac{5}{4H_b^0}\frac{\partial H_b'}{\partial y}\times\sin\left(2\theta_b^0\right)+\frac{r}{\beta}\cos\left(\theta_b^0\right)\frac{\partial^2 H_b'}{\partial y^2}\right) \tag{7}$$

readily follows from the linearized Eqs. (1) and (2). This equation reduces to the classical one-line equation

$$\frac{\partial x_s}{\partial t}=\varepsilon_{cla}\frac{\partial^2 x_s}{\partial y^2} \tag{8}$$

with

$$\varepsilon_{cla}=\frac{2\mu}{\bar{D}}\left(H_b^0\right)^{5/2}\cos\left(2\theta_b^0\right) \tag{9}$$

if the perturbations in wave angle and wave height are neglected (Falqués, 2003): $\theta_b'=0$, $H_b'=0$. Notice that the governing equation, in contrast with Eq. (8), is non local. This means that $\partial x_s(t)/\partial t$ at a particular location $y=y_1$ can not be determined only from $x_s(t)$ and its y-derivatives at $y=y_1$ This is because $\partial x_s(y,t)/\partial t$ depends on the evaluation of θ_b', H_b' and the latter quantities depend on the integration of $\theta'(x,y,t)$, $H'(x,y,t)$ in all the nearshore domain which in turn depends on the values of $x_s(y,t)$ for all y through the perturbed bathymetry.

By considering that any initial perturbation can be expanded in Fourier modes, the behaviour of the individual wave-like disturbances permits to reconstruct the dynamics of arbitrary perturbations because of the linearity of Eq. (7). Therefore, we will hereinafter consider perturbations of the form:

$$x_s(y,t)=Ae^{\sigma t+imy}+c.c. \tag{10}$$

with the associated perturbation in the bathymetry

$$D=D_0(x)-\hat{h}(x)e^{\sigma t+imy}+c.c. \tag{11}$$

where the bathymetric perturbation is given by $\hat{h}(x)=\beta A f(x)$ and $m=2\pi/\lambda$ is the alongshore wavenumber. Similar expressions are assumed for the wave quantities and by inserting these expressions in Eq. (7) the growthrate σ can be computed as:

$$\sigma=-2m\frac{\mu}{\bar{D}}\left(H_b^0\right)^{5/2}\left\{\left(m+i\frac{\hat{\theta}_b'}{A}\right)\cos\left(2\theta_b^0\right)+\left(\frac{rm}{\beta}\cos\left(\theta_b^0\right)+\frac{5i}{4H_b^0}\sin\left(2\theta_b^0\right)\right)\frac{\hat{H}_b'}{A}\right\} \tag{12}$$

where θ_b' and $\hat{H}_b'$ are known after solving the linearized version of (3) over the topography defined by (11). The imaginary part of the growth rate, σ_i, provides the alongshore celerity of each wave-like disturbance:

$$V(m)=-\frac{\sigma_i(m)}{m}. \tag{13}$$

The sign of the real part of the growthrate, σ_r, indicates whether the perturbation will grow (instability) or decay (stability). In case of stability, by comparison with Eq. (8), the 'diffusivity' felt by each wave-like solution will be:

$$\epsilon(m)=-\frac{\sigma_r(m)}{m^2}. \tag{14}$$

Notice that even though the governing equation is not an advection–diffusion one, a wavelength dependent celerity and diffusivity can still be defined by Eqs. (13) and (14).

3.2. Stability under a wave climate

Given a shoreline disturbance it can be expanded by Fourier and each Fourier mode will evolve independently of the rest because of the linearity of the governing equations. The time evolution of the mode with wavenumber m will be defined by Eq. (12) where the complex growth rate σ depends on the wave angle θ_∞, height H_∞ and period T. Thus, its amplification and migration during a time period Δt_1 where wave conditions remain constant, H_1, θ_1, T_1, is given by the factor

$$e^{\sigma(\theta_1,H_1,T_1)\Delta t_1}. \tag{15}$$

In case of a sequence of wave conditions $(H_1,\theta_1,T_1)\ldots(H_n,\theta_n,T_n)$ during the time intervals $\Delta t_1\ldots\Delta t_n$, the overall amplification and migration factor of the mode with wavenumber m during the total time $\Delta t=\sum_{j=1}^{n}\Delta t_j$ will be

$$e^{\sum_{j=1}^{n}\sigma_j\Delta t_j} \tag{16}$$

since the wavenumber m remains the same as time goes on. This is obviously a consequence of the linearity of the governing equation as shoreline features are assumed of small amplitude. As a result, there are no chronology effects, i.e., the final state does not depend on the ordering of the various wave conditions.

Consider now a wave climate with a relative frequency or probability of occurrence $p_j=\Delta t_j/\Delta t$ for each wave conditions (H_j,θ_j,T_j). The amplification and migration factor during the total time Δt will be:

$$e^{\sigma\Delta t} \tag{17}$$

where the resulting complex growthrate is:

$$\sigma=\sum_{j=1}^{n}p_j\sigma_j. \tag{18}$$

From the complex growthrate, the growthrate and the migration celerity are immediately found.

4. Model application to the Dutch coast

The stability of the coast depends on the topography in the basic state, $D_0(x)$, the shape function of the topographic perturbation, $f(x)$ and the wave climate. Regarding the basic topography a Dean profile with a small horizontal shift was

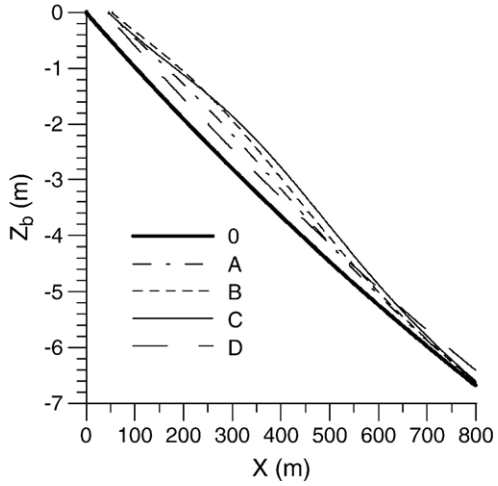

Fig. 2. Equilibrium beach profile (0) and cross-shore bathymetric profiles of the shoreline sand waves at the crest for a horizontal amplitude of 50 m (A, B, C, D). (D) shows the shift of the equilibrium profile, Eq. (20) and (A), (B) and (C) correspond to Eq. (21). (A) with x_m=200 m, L=300 m and a=0.006, (B) with x_m=200 m, L=300 m and a=0.01, (C) with x_m=300 m, L=300 m and a=0.01.

used for the general study in Falqués and Calvete (2005). However, this can not be applied to the Dutch coast since the Dutch inner shelf is very shallow. Indeed, if the shoreline slope and the distance of the depth of closure are prescribed, the 'deep water depth' at a few kilometers from the coast is much larger than the actual one on the Dutch inner shelf. Thus, a better fit is obtained with a profile

$$D_0(x) = \alpha\left(1 - e^{-\beta x/\alpha}\right) \tag{19}$$

where β is the slope at the coastline and α is a constant which is chosen in order to have a prescribed water depth D_∞ at an offshore location x_∞.

Regarding the shape function of the topographic perturbation, two options will be examined. The first one is the assumption that when the shoreline shifts seaward (landward) due to a sand wave, the whole equilibrium profile shifts seaward (landward). This means (Falqués and Calvete, 2005)

$$f(x) = \frac{1}{\beta}\frac{dD_0(x)}{dx} = e^{-\beta x/\alpha}. \tag{20}$$

Another option is the assumption of a cross-shore profile with a maximum perturbation at some offshore location rather than at the shoreline (see Fig. 2). This is achieved with the function

$$f(x) = \left(1 + axe^{-((x-x_m)/L)^2}\right)\left(\frac{e^{-x/x_c} - e^{-1}}{1 - e^{-1}}\right) \tag{21}$$

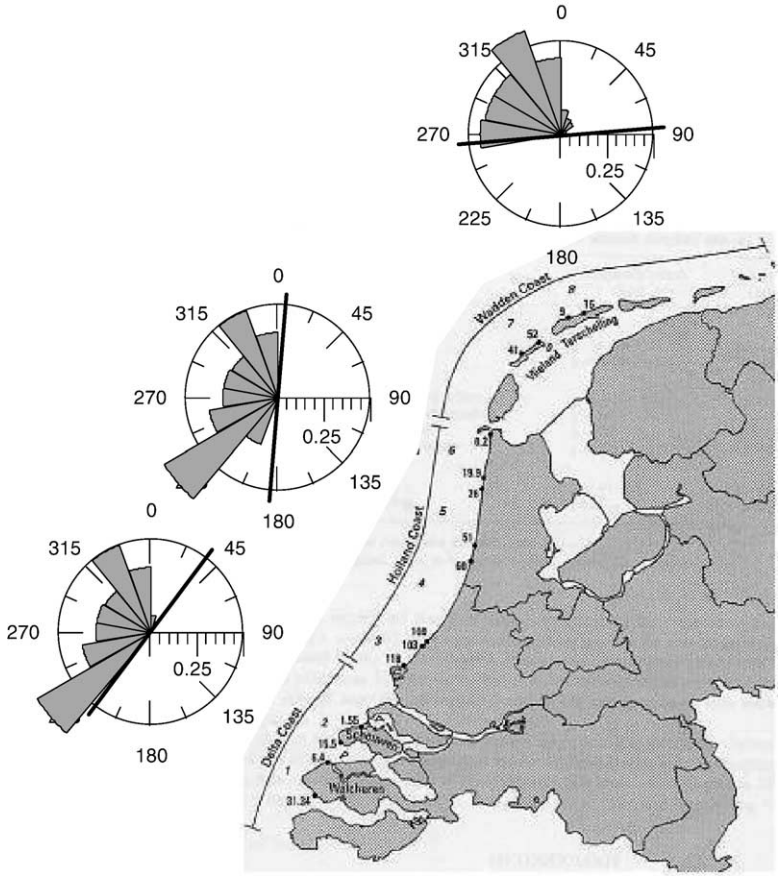

Fig. 3. Map of the Dutch coast (adapted from Ruessink and Jeuken (2002)). The directional distribution of the 'mean annual wave strength' corresponding to each wave direction, $\mathcal{T}(\theta) = \sum_j p(\theta, H_j) H_j^{5/2}$, where $p(\theta, H_j)$ is the probability of waves from the angle θ with significant wave height H_j, is also shown for each section of the coast. The thick lines indicate the mean orientations of the coastline taken for each section.

up to $x=x_c$ and 0 beyond. For $a=0$, this gives a profile similar to that used in (Falqués and Calvete, 2005). For $a\neq 0$, the magnitude of the perturbation can be increased around $x=x_m$ and, for sufficiently large α a bell-shape maximum with a cross-shore width defined by L can be obtained.

The wave climate has been taken from the National Institute for Costal and Marine Management/RIKZ (Golfklimaat web site). For the Wadden coast (northern part, see Fig. 3) the ELD station ($x_\infty=1.5\times10^4$ m, $D_\infty=26$ m) has been used. The Ijmuiden station ($x_\infty=3.6\times10^4$ m, $D_\infty=22$ m) has been used for the central (Holland) and southern (Delta) coasts. The incidence angles and significant wave heights have been divided into 20° and 1 m intervals. A probability of occurrence P_j and a mean wave period T_j were assigned to each bin characterized by a θ_∞ and a $(H_s)_\infty$ intervals. In order to ease the interpretation of the results, the relative strength on annual average of the waves coming from different directions is represented in Fig. 3. Since the sediment transport Q is proportional to $H_b^{5/2}$, this is done by means of the quantity $T(\theta)=\sum_j p(\theta,H_j)H_j^{5/2}$ where H_j is the significant wave height in deep water. Notice that this is just for the interpretation of the results, not for the computations in which the waves are transformed over the curvilinear depth contours from deep water up to breaking. Otherwise, the slightly different power $H_j^{12/5}$ would be more accurate (Ashton et al., 2003). It is also important to note that the present approach is different from the latter paper since the sediment transport in that paper is actually computed as proportional to $H_j^{12/5}$.

5. 'Coastline perturbations'

We first consider perturbations corresponding to a cross-shore shift of the equilibrium profile which decay offshore according to Eq. (20).

5.1. Stability and diffusivity

The growthrates for λ between 3 and 15 km are shown in Fig. 4. It is seen that all sand waves tend to decay, any stretch of the coastline being HAWI stable. The southern part is the most stable while the northern part is a little less stable. Typical decay times, e.g. for $\lambda\sim7$ km., are about 3 yr. Fig. 4 also shows the mean annual diffusivity affecting coastline features as a function of their alongshore length scale, λ. It is seen that the diffusivity is fairly independent of λ for λ larger than about 5 km. Thus, despite its complexity, the governing equation, Eq. (7), behaves like an (advection−) diffusion equation for large scale perturbations. The corresponding diffusivity is about $0.01-0.012$ m^2 s^{-1}. It is also seen that the diffusivity increases substantially for smaller scale perturbations indicating a clear deviation with respect to the behaviour of an advection-diffusion equation.

The model results can be compared to the diffusivity predicted by the classical one-line model given by Eq. (9). The mean annual H_{rms} at the ELD and the YM6 stations are 0.91 and 0.87 m, respectively. The traditional one-line model uses the depth of closure as the average active water depth, $\bar{D}=D_c$ which can thereby be approximated by 8 m at the Delta and Holland coasts, and by 9 m at the Wadden coast. Application of Eq. (9) with $\theta_b\simeq0$ then gives the same diffusivity, $\varepsilon_{cla}\simeq0.026$ m^2 s^{-1}, for the three portions of the Dutch coast. In the range where the diffusivity does not depend on the wavelength (λ above $\simeq5$ km) the model predictions are smaller by a factor 2 on the Delta and Holland coasts and by a factor 2.6 on the Wadden coast. For smaller wavelengths the diffusivity increases and, at some point, the model and the classical predictions coincide. This occurs for $\lambda\simeq1.5$,1.8 and 1 km for the southern, central and northern coasts, respectively. Thus, the traditional one-line model gives a reasonable estimate of the shoreline diffusivity for short length scales 1–2 km. but significantly overpredicts it for larger length scales. This is consistent with the analysis for a generic coast in Falqués (2003) and Falqués and Calvete (2005).

The directional contribution of the wave climate to the mean annual diffusivity is shown in Fig. 5. For the Delta coast, it is seen that the waves coming from the SW give a negative contribution, that is, cause shoreline instability. It is found in Falqués and Calvete (2005) that high waves (with respect to the

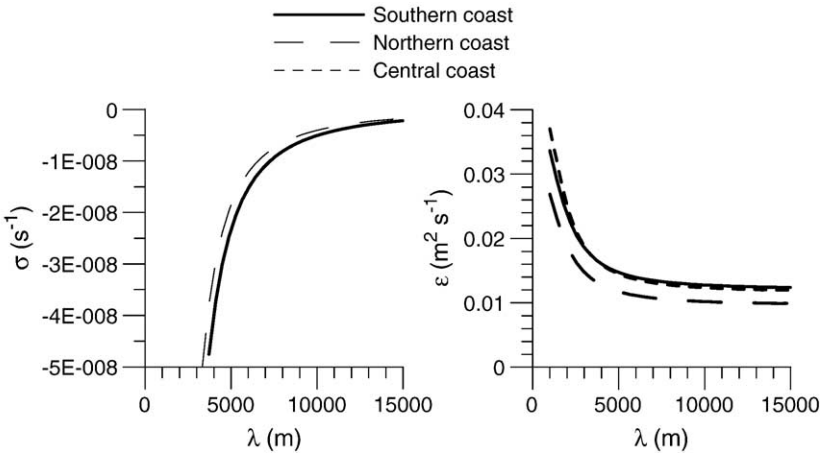

Fig. 4. Left: Predicted growth rate of the HAWI on the Dutch coast as a function of the wavelength of the coastline waves. Right: annual mean diffusivity of coastline perturbations as a function of wavelength. The cross-shore profile of the topographic perturbation is given by Eq. (20).

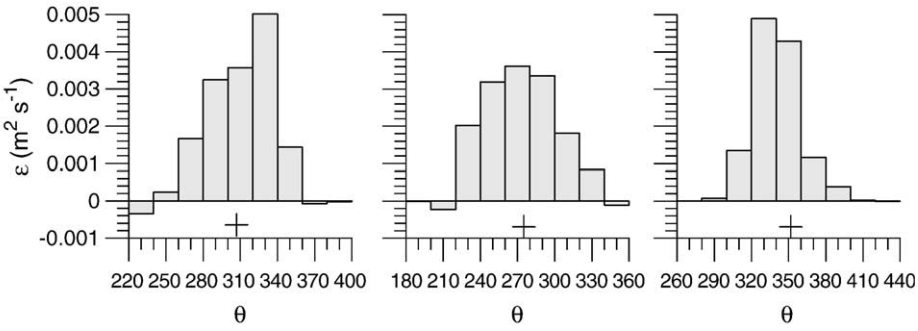

Fig. 5. Directional contribution of the wave climate to the mean annual diffusivity of coastline features along the Dutch coast for a wavelength $\lambda = 5$ km. The bathymetric perturbation is given by a shift of the equilibrium profile, Eq. (20). The angle is with respect to North. The shore normal direction for each portion of the coast is indicated by a cross. Left: Delta coast; center: Holland coast; right: Wadden coast.

highest in the wave climate) with large periods do not produce instability even for high incidence angles. In this case, however, the high obliqueness in combination with the relative short periods lead to instability even if the waves from the SW are commonly high, representing a very large contribution to the annual wave energy (see Fig. 3). As can be seen, the negative diffusivity induced by the SW waves is overwhelmed by the positive diffusivity induced by the waves coming from other directions. The most significant positive contribution comes from the N–NW. This is not surprising as the obliqueness is relatively low, these waves also represent a very large portion of the annual wave energy (Fig. 3) and they have periods which are slightly larger than those from the SW.

The situation is somewhat different for the Holland coast. Now, the waves from the SW are less oblique due to the different trend of the coast (Fig. 3) and they cause stability. The waves from the N–NW contribute also with positive diffusivity but much less than for the Delta coast because their obliquity is larger. However, the angle of about 55° is not high enough to cause instability probably due to the large wave height and period of such waves (it is shown in Falqués and Calvete (2005) that the threshold angle for HAWI is in general larger than that found by Ashton et al. (2001), ~42°). For the Holland coast there is a very small contribution to instability from the S–SW waves and from the N waves. The contributions to stability coming from less oblique waves are however much larger and the coast is overall stable. It is also interesting to note that the contribution to positive diffusivity is more evenly distributed in contrast to the Delta coast where the N–NW waves are clearly the main contribution to coastline diffusivity.

Finally, it turns out that the Wadden coast is clearly dominated by N–NW and N waves that renders it stable due to the almost normal incidence. Apparently, there is no significant contribution to instability from any approach direction. This is probably due to the fact that the high angle waves on this coast are not energetic enough (see Fig. 3) to produce a significant contribution with negative diffusivity.

Fig. 5 shows that there is a tendency to instability of the Delta coast due to SW waves. This is clearly corroborated by an experiment where all the waves in the annual wave climate have been assumed to approach from the SW. As it can be seen in Fig. 6, the coastline would then be unstable with a linearly dominant wavelength of 6.3 km and a growth time of 21 yr. Thus, the spreading of angles on the real wave climate renders the coast stable and we conclude, in agreement with Ashton et al. (2003), that the main reason for coastline stability is the insufficient wave obliqueness.

5.2. Shoreline sand wave propagation

As shown in the last section, HAWI can not generate alongshore sand waves on the long term, i.e., on a time scale of years. However, if such waves were generated by whatever reason, the model describes its propagation celerity according to Eq. (13). Fig. 7 shows the celerity of sand waves for λ between 3 and 15 km. It is found that the migration celerity decreases with increasing wavelength. Both the sand waves along the Delta coast and along the Wadden coast migrate to the north/northeast and on the latter they do with a larger celerity. On the central coast they migrate also to the north but with much smaller celerity. In the latter case it is found that small changes in model conditions (e.g., profile of the topographic perturbation) can reverse the migration celerity. This is fully consistent in a qualitative sense with the data analysis of Ruessink and Jeuken (2002). But also the quantities are close to observations in case of the southern and the northern stretches of coast. Model predictions are within the correct order of magnitude for the observed range of wavelengths. For instance, in case of $\lambda = 7$ km, the celerities

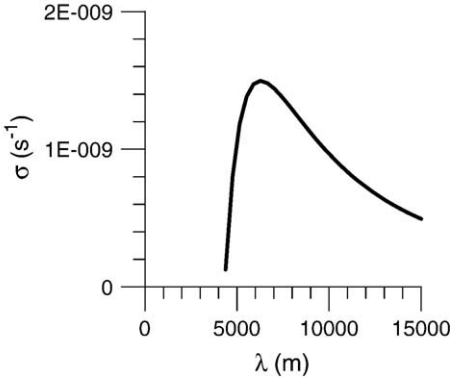

Fig. 6. Growth rate curve as a function of wavelength for HAWI on the Delta coast under the assumption of all the waves approaching from the SW.

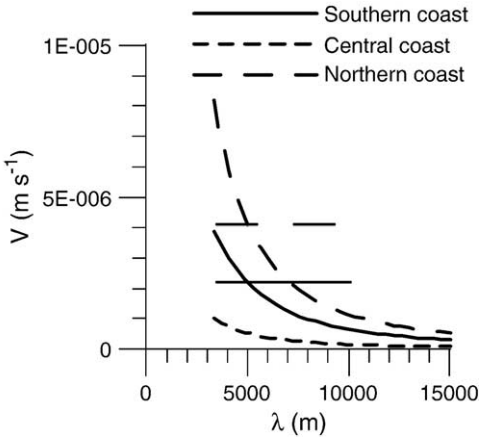

Fig. 7. Northward/northeastward migration celerity of the shoreline sand waves along the Dutch coast as a function of their wavelength. The thin horizontal lines correspond to the observed celerities along the southern coast (0.07 km/yr) and the northern coast (0.13 km/yr).

are 0.039 km/yr and 0.071 km/yr for the Delta and the Wadden coasts, respectively. But even a perfect agreement of 0.070 and 0.13 km/yr is attained in case of $\lambda = 5$ km. This is remarkable given the large number of simplifications of the model and the fact that no parameter tuning has been done. For instance, the constant μ in front of the CERC formula, Eq. (2), has been fixed to 0.15 $m^{1/2}$ s^{-1} which is well in the center of the accepted interval. For the Holland coast the predicted celerity is 0.016 km/yr in case of $\lambda = 5$ km. This small value and the fact that it can be even reversed by changing model conditions is also consistent with observations according to which there is no clear propagation direction along this section of the coast.

A similar directional analysis to that done for the diffusivity yields insight into the reasons for the observed propagation. On the Delta coast, both the SW and the N–NW waves are the main cause of propagation to the NE and to the SW, respectively. It is seen in Fig. 8 that probably due to the higher obliquity of SW waves, their contribution is dominant with the result that the annual mean propagation is to the NE. In contrast, it is remarkable that on the Holland coast, although the celerities to the NE or to the SW caused by the waves from the SW or from the N–NW are larger than on the southern coast, they are almost balanced. This would be the reason why there is no clear propagation direction on the long term in this part of the coast.

On the Wadden coast there is a net propagation to the NE which is driven by the waves approaching from the W to the N–NW directions. Their contribution is rather small since they either are not very energetic or they are not very oblique (see Fig. 3). It is seen that their contribution to NE propagation is comparable or even smaller than that of the waves driving NE propagation on the Delta or Holland coast. Amazingly, however, the fastest NE propagation is observed on that coast. It is seen in Fig. 8 that this is due to the extremely weak SW propagation caused by waves from the N to the E–NE directions which are typically very mild (see also Fig. 3).

6. 'Offshore perturbations'

As it is shown in Falqués and Calvete (2005), High angle waves instability depends on the offshore extent of the bathymetric perturbation associated with shoreline features. Similarly, it also depends upon the shape of the bathymetric perturbation. While there is information of the Dutch coastline position during the last 150 years, there is no detailed data on the bathymetry during such a period of time. Thus, something has to be assumed for the bathymetric structure of the sand waves. It is reasonable to assume that the whole equilibrium profile just shifts seaward or landward at the crest or the trough of a sand wave, respectively. Strictly speaking, this is incompatible with the concept of depth of closure (see Falqués and Calvete (2005)) since in this case there is a bathymetric perturbation which decays offshore but which extends up to infinity, i.e., beyond the depth of closure. However, it is a quite natural assumption and has been adopted in Section 5 (Eq. (20)) as a first test. It has been seen in that section that the Dutch coastline is stable under such an assumption with the result that HAWI can not be considered as a possible cause of the shoreline sand waves along this coast.

It is therefore an interesting exercise investigating whether the assumption of a different bathymetric perturbation associated with the sand waves could render the coastline unstable. Thus, we consider now a cross-shore profile with a shape function given by Eq. (21) that is maximum at some distance from the coastline. We explore three different sets of para-

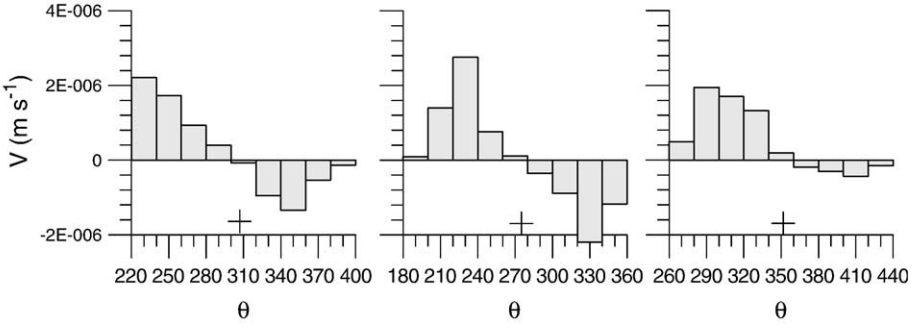

Fig. 8. Directional contribution of the wave climate to the mean annual alongshore propagation of coastline features along the Dutch coast for a wavelength $\lambda = 5$ km. Positive (negative) values indicate NE (SW) propagation. The bathymetric perturbation is given by a shift of the equilibrium profile, Eq. (20). The angle is with respect to North. The shore normal direction for each portion of the coast is indicated by a cross. Left: Delta coast; center: Holland coast; right: Wadden coast.

meters, A (x_m=200 m, L=300 m, a=0.006), B (x_m=200 m, L=300 m, a=0.01) and C (x_m=300 m, L=300 m, a=0.01). As can be seen in Fig. 2, these profiles would correspond to relatively subtle transverse bars attached to the crests with the opposite bed depressions in front of the embayments. The maximum bed level perturbation associated with these bars would be located within the surf zone for moderate storm waves of about H~3 m.

6.1. Stability

As can be seen in Fig. 9 (left), in case of profile C the Delta and the Holland coasts become now unstable with dominant wavelengths of about 5.5 and 4.5 km, respectively. The typical growth times are of 9 and 2.9 years, respectively. The Wadden coast becomes slightly unstable, with a growth time of 49 years for a dominant wavelength of 8 km. These wavelengths are consistent with observations which also show larger wavelengths on the northern coast than on the southern and central coasts. In contrast, for profiles A and B, the coastline remains stable. This is remarkable since profiles B and C are very similar, the only difference being that the bathymetric perturbation in B is located slightly more onshore. In case of B, typical decay times for a wavelength of 5 km are about 3.6 and 2.5 yr on the Delta, Holland and Wadden coasts, respectively.

The reasons for instability/stability can be understood looking at the coastline diffusivity in Fig. 10. The structure of the histograms is relatively similar to those in Fig. 5 but where all the diffusivities have been shifted quite uniformly towards negative values (instability). The Delta coast is unstable mainly due to the SW waves whereas both the SW and the N–NW waves have a similar influence on the Holland coast instability. As it is seen in Fig. 9, the overall effect is that the Holland coast is more unstable than the Delta coast. On the Wadden coast, there is an important contribution to instability of the waves from the W–NW but it is nearly balanced by the strong stabilizing effect of the N–NW waves which approach the coast with very small angle. However, even if the waves from the NE and E–NE are rather mild they have a high angle with the result that the overall effect is a weak instability.

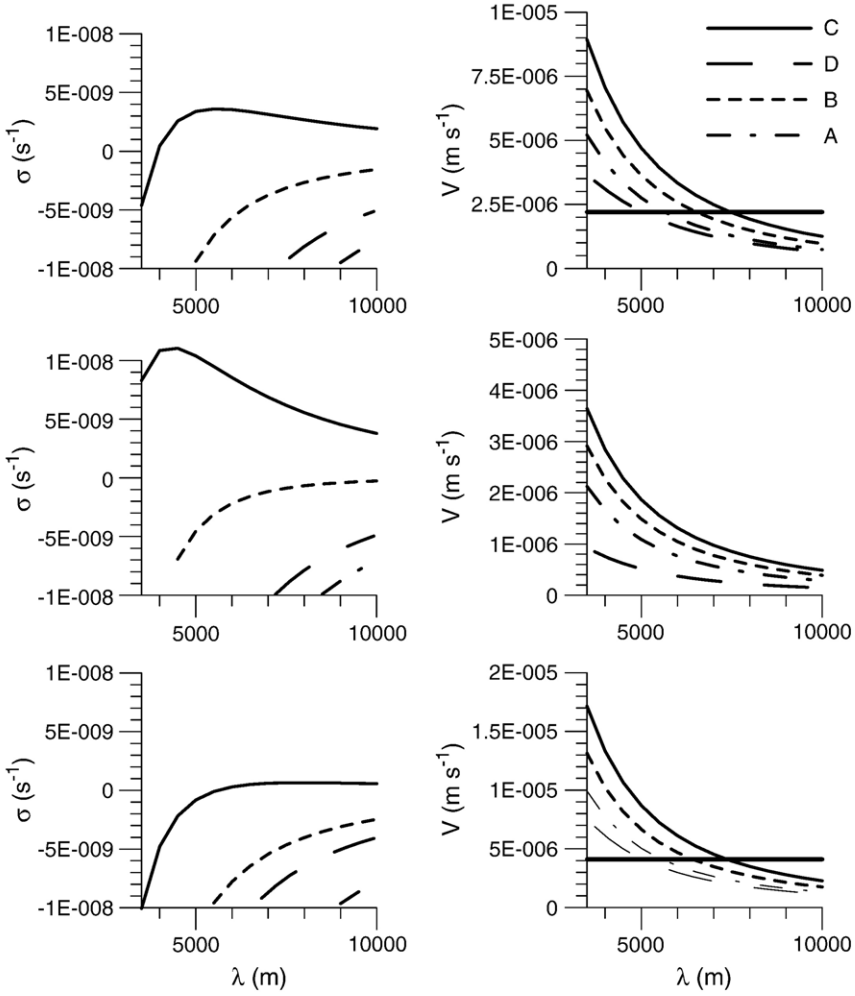

Fig. 9. Sensitivity of growthrates and migration celerities to cross-shore sand wave profiles. The different lines indicated by A, B, C and D correspond to Fig. 2. Growthrates on the left and celerities on the right. Upper plots correspond to the southern coast, middle plots to the central coast and bottom plots to the northern coast. The horizontal lines on the plots on the right indicate the observed celerity on the southern (0.07 km/yr) and northern (0.13 km/yr) coasts.

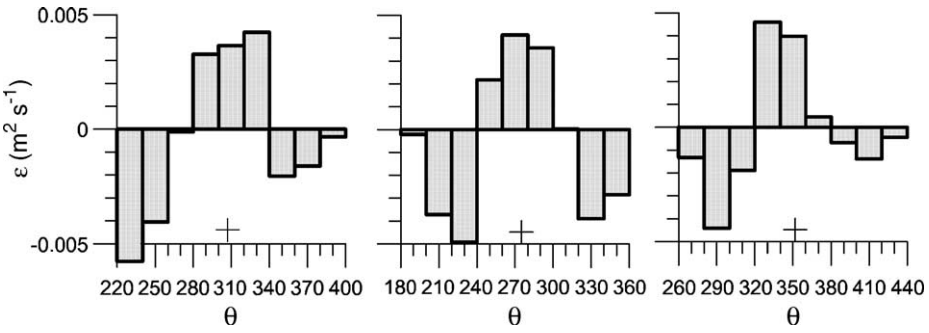

Fig. 10. Directional contribution of the wave climate to the mean annual diffusivity of coastline features along the Dutch coast under the assumption that the maximum bathymetric signal is at some distance from the shore (Eq. (21), profile C). The angle is with respect to North. The shore normal direction for each portion of the coast is indicated by a cross. Left: Delta coast, $\lambda = 5.5$ km; center: Holland coast, $\lambda = 4.5$ km; right: Wadden coast, $\lambda = 8$ km.

6.2. Shoreline sand wave propagation

Fig. 9 (right) shows the sand wave celerities for the range of wavelengths observed by Ruessink and Jeuken (2002) along the Dutch coast and by using profiles A, B and C. Profile D (shift of the equilibrium topography) is also included. The observed celerities which are about 0.07 and 0.13 km/yr along the southern and northern coasts are also indicated. It is seen that a maximum of the bathymetric perturbation away from the shoreline systematically increases the celerity. For each predicted celerity, the intersect of the model curve with the observed value occurs for certain wavelength. Interestingly, even if there is variability due to the uncertainty on the profile, the wavelengths of coincidence between model and observations are between 5 and 7.8 km, i.e., well within the range of observed wavelengths which is 3.5–10 km. The results for the center coast are less encouraging. For the 7 km wavelength profile C gives a celerity of 0.03 km/yr instead of 0.009 km/yr with profile D. This is too high since observations indicate that there is no clear overall migration direction in that section of the coast. Anyway, it is still true that the predicted celerity along the Holland coast is a factor 2.6 smaller than along the Delta coast and a factor 4.6 smaller than along the Wadden coast (for the 7 km wavelength).

7. Discussion

The results presented in Section 6 show that the southern and central parts of the Dutch coast could be HAWI unstable if the coastline sand waves were associated with offshore shoals with a maximum bathymetric perturbation away from the coast. The results regarding stability or instability are very sensitive to the cross-shore shape of such perturbations, especially to its offshore extension. It is known that the Dutch shoreline sand waves have a significant offshore signal since they are capable of bypassing long jetties (O(km)) on the coast (Verhagen (1989) and personal communication). Thus, the alongshore sediment transport would render the Dutch coast unstable with respect to some of those perturbations.

The problem would then be by which reason the cross-shore sediment transport feeds such perturbations rather than just shifting the equilibrium profile. One could think of shore-parallel bars with an alongshore rhythmicity which are quite common on the Dutch coast (Guillen et al., 1999; van Enckevort et al., 2004). Yet the alongshore rhythmicity of crescentic bars is at most 2–3 km (Guillen et al., 1999; van Enckevort et al., 2004), that is, at least twice smaller than the HAWI dominant wavelength. Looking at profile C which is the one that produced instability, it is interesting to realize that the maximum bathymetric perturbation is close enough to the coast to be considered inside the surf zone in case of moderate storm waves. Thus, the shoreline sand waves could result from the cross-shore redistribution of the sand associated with an alongshore series of shoals and bed depressions generated by the alongshore transport in the surf zone for storm waves. Therefore the Dutch coast has potential for high angle-waves instability.

The sensitivity to the shape of the bathymetric perturbations is also found in the migration celerities. This sensitivity is however not qualitatively important. First, for the southern and northern coasts, the wavelength for which model and observations coincide is always well within the range of the observed wavelengths. Second, for a given wavelength and for any profile, the celerity along the northern coast is larger than the one along the southern coast and this one larger than the one along the center coast. This is again consistent with the observations.

Since the shifting from stability to instability originated by small changes in the sand wave profile could be overall interpreted as the coast being at the threshold for instability, the present results would be in line with previous research by Ashton et al. (2003). As this paper uses the CERC formula instead of Eq. (2), some tests have been done to check possible important differences in both studies due to the term $\partial H_b/\partial y$. It has been found that this term is slightly stabilizing and produces a small increase in celerity. The effects are however rather small, a maximum reduction about 7% in growthrates and a maximum increase about 14% in celerities.

Additional comparison with Ashton et al. (2003) is worth pursuing. Although their 'instability indexes' are negative along all the coast, they are nearly 0 for some stretches along the Holland coast. This is clearly consistent with our results according to which this section is the most potentially unstable. Although there is stability on average, sand waves originated during periods of wave conditions favorable to instability can last for a very long time until they eventually decay, especially

in those stretches where the instability index is nearly zero. Such waves along the southern part of the Holland coast (their Section 3) may have wavelengths of about 4 km, which are rather close to the present prediction. This is intriguing, as the wavelength selection mechanism in Ashton et al. (2003) is fully related to nonlinear effects, something missing in the present model. The physics of the sand wave propagation is totally different too in both models, relaying again on nonlinear effects in Ashton et al. (2003). This model does not predict migration along the Wadden coast while the maximum celerity is observed on that coast. From Fig. 5 (3) of that paper, the celerity for the Delta coast could be inferred to be about 0.15 km/yr, twice the observed one. Thus, the present model gives a much better prediction on these sections of the coast. In contrast, no propagation or slightly southward propagation is obtained by Ashton et al. (2003) on the Holland coast which is more successful prediction than the present one.

8. Conclusions

It has been found that the dominance of the waves approaching from the SW and from the NW/N together with the mean cross-shore bathymetric profile render the Delta and Holland coastlines potentially unstable. This is less pronounced on the Wadden coast where the latter waves approach the coast almost normally and cause a strong diffusive effect. Whether this instability actually occurs or not in the model depends on the assumptions on the cross-shore profile of the bathymetric perturbations. Under the sensible assumption that the maximum bathymetric signal of the shoreline sand waves is at the coastline, the Dutch coastline is stable. However, if the longshore transport in the surf zone in case of storm waves together with the redistribution of sediment due to cross-shore transport would produce a maximum bathymetric perturbation away from the coastline, the Delta and Holland coasts could be unstable. For the example that has been worked out in this study, the emerging wavelength would be about 5.5 and 4.5 km, respectively, which is inside the range of observed wavelengths. The growth times would be about 2.9 and 9 years.

The model computations have also implications on the diffusivity experienced by shoreline features in case of stability. Since the governing equation is not a diffusion one, the 'diffusivity' depends on the alongshore wavelength of the Fourier components of such features. Under the assumption that the bathymetric signal of such features is just a cross-shore shift of the equilibrium profile, the diffusivity for the wavelengths above some 5 km is almost independent of λ and is about 0.010–0.015 $m^2\ s^{-1}$. This is roughly half the one that would be predicted by the traditional one-line model with the mean annual wave height on the Dutch coast. This is fully consistent with the general analysis in Falqués (2003) and Falqués and Calvete (2005) according to which the traditional model tends to overpredict coastline diffusivity. However, the diffusivity increases for decreasing λ so that in the range $\lambda \simeq 1$–2 km, the model predictions are similar to those of the traditional model.

No matter the sand waves grow (instability) or decay (stability), a robust feature of the model is that they clearly propagate to the NE or to the E–NE along the Delta and the Wadden coasts on an annual average. On the Holland coast, the model predicts a weak northward migration. The migration celerities increase with decreasing wavelength. In spite of the sensitivity to the unknown cross-shore profile of the sand waves, the model predictions are in a perfect qualitative agreement with observations, according to which the propagation is faster along the Wadden coast than along the Delta coast whereas it is unclear along the Holland coast. The reasons for such a behaviour on the Delta and Holland coasts is a competition between SW and NW/N waves. Due to the orientation of the Holland coast, the effect of such waves are almost balanced on (annual) average so that the mean propagation is very weak or vanishing. In contrast, this balance is broken on the Delta coast. The obliquity of SW waves with respect to this coast is higher than that of the NW/N waves with the result that there is an annual mean propagation to the NE. The situation is very different on the Wadden coast where the maximum migration celerity is observed. This occurs, not because the waves approaching from the directions ranging from the W to the N–NW produce a very strong effect, but because the opposing effect of the waves coming from the N–NE to the E–NE is very weak. The quantitative results are encouraging on the Delta and Wadden coasts since despite the sensitivity to the profiles the wavelength at which model and observations coincide is well within the range of observed wavelengths. Less satisfactory is the fact that a (small) northward propagation is found for the Holland coast while observations show either stationary waves or occasional propagation to the north or to the south.

The present model results have the limitation of being based on a cross-shore profile of the sand waves which is not yet known from observations. However, after some sensitivity analysis to the profiles, a good description of the propagation of shoreline sand waves along the Dutch coast is found. It is also indicated that the Dutch coast is potentially unstable due to high angle-waves. Whether the instability occurs or not depends on the profile of the sand waves but it is shown that it actually occurs in cases with sensible assumptions on it. The final conclusion is that the instability and propagation driven by the wave-driven alongshore sand transport could be the origin of such waves. However, to elucidate whether this is really the case would require further work, both theoretical and experimental. This should include model refinement to account for cross-shore profile dynamics and checking the link between coastline waves and offshore shoals in field observations. On the other hand, the shoals related to tidal inlet dynamics have been suggested as the cause of such shoreline waves (Bakker, 1968; Ruessink and Jeuken, 2002). Since HAWI on the Dutch coast needs a significant offshore signal of the sand waves, these shoals could trigger the instability. Thus, it is conceivable that such waves could obey to some interaction free-forced behaviour related to alongshore wave-driven sediment transport and tidal inlet dynamics.

Acknowledgments

This research is part of the HUMOR project, funded by the European Commission under Contract No. EVK3-2000-22014-HUMOR. Partial funding from the Spanish Ministerio de Ciencia y Tecnología through the PUDEM project under contract REN2003-06637-C02-01/MAR is also gratefully acknowledged. This work has been partly carried out during a sabbatical stay of the author at the IMAU (University of Utrecht). The author likes to thank Dr. Huib E. de Swart and his Coastal Group for their support and inspiring discussions during that period. Thanks are also due to the National Institute for Costal and Marine Management/RIKZ (The Netherlands) for providing information on the Dutch wave climate.

References

Ashton, A., Murray, A.B., Arnault, O., 2001. Formation of coastline features by large-scale instabilities induced by high-angle waves. Nature 414, 296–300.

Ashton, A., Murray, A.B., Ruessink, G.B., 2003. Initial tests of a possible explanation for alongshore sandwaves on the Dutch coast. In: Sánchez-Arcilla, A., Bateman, A. (Eds.), Proc. 3rd IAHR Symposium on River, Coastal and Estuarine Morphodynamics, vol. 1, pp. 320–330. Barcelona, Spain.

Bakker, W.T., 1968. A mathematical theory about sand waves and its application on the Dutch Wadden Isle of Vlieland. Shore Beach 36, 4–14.

Bruun, P., 1954. Migrating sand waves or sand humps, with special reference to investigations carried out on the Danish North Sea coast, in coastal England. Am. Soc. Civ. Eng., Grenoble, France, 269–295.

Falqués, A., 2002. Shoreline sand waves. Survey of available data., Tech. rep., HUMOR project, Grup de Morfodinàmica de Costes, Appl. Physics Dept., Univ. Politècnica de Catalunya, Barcelona, Spain.

Falqués, A., 2003. On the diffusivity in coastline dynamics. Geophys. Res. Lett. 30, 2119.

Falqués, A., Calvete, D., 2005. Large scale dynamics of sandy coastlines. Diffusivity and instability. J. Geophys. Res. 110.

Guillen, J., Stive, M.J.F., Capobianco, M., 1999. Shoreline evolution of the Holland coast on a decadal scale. Earth Surf. Processes. Landf. 24, 517–536.

Horikawa, K., 1988. Nearshore Dynamics and Coastal Processes. University of Tokio Press, Tokio, Japan.

Inman, D.L., 1987. Accretion and erosion waves on beaches. Shore Beach 55, 61–66.

Komar, P.D., 1998. Beach Processes and Sedimentation, second ed. Prentice Hall.

Larson, M., Kraus, N.C., 1991. Mathematical modeling of the fate of beach fill. Coast. Eng. 16, 83–114.

Larson, M., Hanson, H., Kraus, N.C., 1987. Analytical solutions of the one-line model of shoreline change. Tech. Rep., US Army Corps of Engineers.

Mei, C.C., 1989. The applied dynamics of ocean surface waves. Advanced Series on Ocean Engineering vol. 1. World Scientific, Singapore.

Pelnard-Considère, R., 1956. Essai de theorie de l'evolution des formes de rivage en plages de sable et de galets. 4th Journees de l'Hydraulique, Les Energies de la Mer, Paris vol. III(1). Société Hydrotechnique de France, pp. 289–298.

Ruessink, B.G., Jeuken, M.C.J.L., 2002. Dunefoot dynamics along the Dutch coast. Earth Surf. Processes Landf. 27, 1043–1056.

Stewart, C.J., Davidson-Arnott, R.G.D., 1988. Morphology, formation and migration of longshore sandwaves; Long Point, Lake Erie, Canada. Mar. Geol. 81, 63–77.

Stive, M.J.F., Aarninkhof, S.G.J., Hamm, L., H.H., Larson, M., Wijnberg, K.M., Nicholls, R.J., Capobianco, 2002. Variability of shore and shoreline evolution. Coast. Eng. 47, 211–235.

Thevenot, M.M., Kraus, N.C., 1995. Longshore sandwaves at Southampton Beach, New York: observations and numerical simulation of their movement. Mar. Geol. 126, 249–269.

van Enckevort, I.M.J., Ruessink, B.G., Coco, G., Suzuki, K., Turner, I.L., Plant, N.G., Holman, R.A., 2004. Observations of nearshore crescentic sandbars. J. Geophys. Res. 109.

Verhagen, H.J., 1989. Sand waves along the Dutch coast. Coast. Eng. 13, 129–147.